ЖЭТФ, 2001, том 120, вып. 2 (8), стр. 470–479

PHASE SEPARATION IN SYSTEMS WITH CHARGE ORDERING

M. Yu. Kagan [a]*, ***K. I. Kugel*** [b], ***D. I. Khomskii*** [c]

[a] *Kapitza Institute for Physical Problems, Russian Academy of Sciences*
117334, Moscow, Russia

[b] *Institute of Theoretical and Applied Electrodynamics, Russian Academy of Sciences*
127412, Moscow, Russia

[c] *Laboratory of Applied and Solid State Physics, Materials Science Center,*
University of Groningen
9747AG, Groningen, the Netherlands

Submitted 25 December 2000

A simple model of charge ordering is considered. It is explicitly shown that at any deviation from half-filling ($n \neq 1/2$), the system is unstable with respect to the phase separation into the charge-ordered regions with $n = 1/2$ and metallic regions with a smaller electron or hole density. A possible structure of this phase-separated state (metallic droplets in a charge-ordered matrix) is discussed. The model is extended to account for the strong Hund-rule onsite coupling and the weaker intersite antiferromagnetic exchange. The analysis of this extended model allows us to determine the magnetic structure of the phase-separated state and to reveal the characteristic features of the manganites and other substances with charge ordering.

PACS: 71.45.Lr, 75.10.-b, 75.30.Mb, 75.30.Kz

1. INTRODUCTION

The problem of charge ordering in magnetic oxides attracts attention of theorists since the discovery of the Verwey transition in magnetite in the end of the thirties [1]. An early theoretical description of this phenomenon was given, e.g., in [2]. This problem was recently reexamined in a number of papers in connection with the colossal magnetoresistance in manganites, see, e.g., [3–5]. The mechanisms stabilizing the charge-ordered state can be different: the Coulomb repulsion of charge carriers (the energy minimization requires keeping the carriers as far away as possible, similarly to the Wigner crystallization) or the electron–lattice interaction leading to the effective repulsion of electrons at the nearest-neighbor sites. In all cases, charge ordering can arise in mixed-valence systems if the electron bandwidth is sufficiently small for the large electron kinetic energy to stabilize the homogeneous metallic state. In real materials, in contrast to the Wigner crystallization, the underlying lattice periodicity determines the prefered types of charge ordering. Thus, in the simplest bipartite lattice, which occurs in the colossal magnetoresistance manganites of the type $R_{1-x}A_xMnO_3$ (where R = La, Pr and A = Ca, Sr) or layered manganites $R_{2-x}A_xMnO_4$, $R_{2-2x}A_{1+2x}Mn_2O_7$, the optimum conditions for the formation of the charge-ordered state exist for the doping $x = 1/2$. At this value of x, the concentrations of Mn^{3+} and Mn^{4+} are equal and the simple checkerboard arrangement is possible. The most remarkable experimental fact here is that even at $x \neq 1/2$ (in the underdoped manganites with $x < 1/2$), only the simplest version of charge ordering is experimentally observed with the alternating checkerboard structure of the occupied and empty sites in the basal plane [6]. In other words, this structure corresponds to the doubling of the unit cell, whereas more complicated structures with a longer period (or even incommensurate structures) do not actually appear in this case.

A natural question then arises as to how the extra or missing electrons can be redistributed for an arbitrary doping level such that the superstructure remains

*E-mail: kagan@kapitza.ras.ru

the same as for $x = 1/2$? To answer this question, the experimentalists introduced the concept of the incipient charge-ordered state corresponding to the distortion of a long-range charge ordering by microscopic metallic clusters [7]. In fact, the existence of this state implies a certain phase separation. We note that the phase separation scenario in manganites is very popular presently [8–15]. There is a growing evidence suggesting that an interplay between the charge ordering and the tendency toward phase separation plays an essential role in the physics of materials with the colossal magnetoresistance.

In this paper, we consider a simple model allowing us to clarify the situation at an arbitrary doping. The model includes both the Coulomb repulsion of electrons on the neighboring sites and the magnetic interactions responsible for the magnetic ordering in manganites. After demonstrating the instability of the system toward phase separation in certain doping ranges, we consider the simplest form of the phase separation — the formation of metallic droplets in the insulating matrix. We estimate parameters of such droplets and construct the phase diagram illustrating the interplay between charge ordering, magnetic ordering, and phase separation.

We note that the charge ordering mechanism considered below (the Coulomb repulsion) is not the only one. The electron–lattice interaction can also play an important role, see, e.g., [16]. In application to manganites, one must also take the orbital and magnetic interactions into account [4, 16, 17]. These may be important, in particular, in explaining the fact that the charge ordering in half-doped perovskite manganites is a checkerboard one only in the basal plane, but it is «in-phase» along the c-direction. However, the nature of this charge ordering is not clear yet and presents a separate problem: it is not evident that the dominant mechanism is indeed given by the magnetic interactions responsible for this stacking of ab-planes in [16]. We also emphasize that the charge ordering is often observed in manganites at higher temperatures than the magnetic ordering, and one must seek a model that does not heavily rely on magnetic interactions. In contrast to magnetic interactions, the Coulomb interaction is one of the important factors that is always present in the systems under consideration. Moreover, it has a universal nature and does not critically depend on specific features of a particular system. Consequently, our treatment can also be applied to other systems with charge ordering such as magnetite Fe_3O_4 [1], cobaltites [18], nickelates [19], etc.

2. THE SIMPLEST MODEL FOR CHARGE ORDERING

We consider a simple lattice model for charge ordering,

$$\hat{H} = -t \sum_{\langle i,j \rangle} c_i^+ c_j + V \sum_{\langle i,j \rangle} n_i n_j - \mu \sum_i n_i, \qquad (1)$$

where t is the hopping integral, V is the nearest-neighbor Coulomb interaction (a similar nn repulsion can also be obtained via the interaction with the breathing-type optical phonons), μ is the chemical potential, and c_i^+ and c_j are one-electron creation and annihilation operators, $n_i = c_i^+ c_i$. The symbol $\langle i, j \rangle$ denotes the summation over the nearest-neighbor sites. Here, we omit spin and orbital indices for simplicity. As mentioned in the Introduction, the spin and orbital effects play an important role in the formation of the real structure in specific compounds; in this section, however, we emphasize the most robust effects related to the nearest-neighbor Coulomb repulsion. The magnetic effects are discussed in Sec. 5. We also assume that the double occupancy does not occur in this model because of the strong onsite repulsion between electrons.

Hamiltonian (1) explicitly accounts for the correlation effect that is most important for the formation of charge ordering, namely, the electron repulsion on neighboring sites. The long-range part of the Coulomb interaction only leads to the renormalization of the bandwidth W and does not significantly affect the properties of the uniform charge-ordered state. However, it can produce a qualitative effect on the structure of the phase-separated state (see the discussion in the beginning of Sec. 4).

The models of type (1) with the nn repulsion responsible for the charge ordering are the most popular ones in describing this phenomenon, see, e.g., [2, 3, 5, 20] and references therein. Hamiltonian (1) captures the main physical effects; if necessary, one can add some extra terms to it, which we do in Sec. 5.

In the main part of this paper, we always speak about electrons. However, in application to real manganites, we mostly have in mind less than half-doped (underdoped) systems of the type $R_{1-x}A_xMnO_3$ with $x < 1/2$. For a real system, one must therefore substitute holes for our electrons. All the theoretical treatment definitely remains the same (from the very beginning, we could define the c and c^+ operators in (1) as the operators of holes); we hope that this does not lead to any misunderstanding.

In what follows, we consider the simplest case of square ($2D$) or cubic ($3D$) lattices, where the simple

two-sublattice ordering occurs for $x = 1/2$. As mentioned in the Introduction, this is the case in layered manganites, whereas in $3D$ perovskite manganites, this ordering occurs only in the basal plane (the ordering is «in-phase» along the c direction). A more complicated model is apparently needed to account for this behavior.

For $n = 1/2$, model (1) was analyzed in many papers; we follow the treatment in Ref. [2]. As mentioned above, the Coulomb repulsion (the second term in (1)) stabilizes the charge ordering in the form of a checkerboard arrangement of the occupied and empty sites, whereas the first term (band energy) opposes this tendency. At arbitrary values of the electron density n, we first consider a homogeneous charge-ordered solution and use the same ansatz as in [2], namely

$$n_i = n[1 + (-1)^i \tau]. \tag{2}$$

This expression implies the doubling of the lattice periodicity, with the local densities

$$n_1 = n(1+\tau), \quad n_2 = n(1-\tau)$$

at the neighboring sites. We note that at $n = 1/2$ for a general form of the electron dispersion without nesting, the charge-ordered state exists only for a sufficiently strong repulsion $V > 2t$ [2]. The order parameter is $\tau < 1$ for finite $V/2t$, and the ordering is not complete in general, i.e., an average electron density n_i differs from zero or one even at $T = 0$.

We use the coupled Green's function approach as in [2], which yields

$$\begin{cases} (E+\mu)G_1 - t_k G_2 - zVn(1-\tau)G_1 = \dfrac{1}{2\pi}, \\ \\ (E+\mu)G_2 - t_k G_1 - zVn(1+\tau)G_2 = 0, \end{cases} \tag{3}$$

where G_1 and G_2 are the Fourier transforms of the normal lattice Green's functions

$$G_{il} = \langle\langle c_i c_l^+ \rangle\rangle$$

for the respective sites i and l belonging to the same sublattice or to different sublattices, z is the number of nearest neighbors, and t_k is the Fourier transform of the hopping matrix element. In deriving (3), we performed a mean-field decoupling and replaced the averages $\langle c_i^+ c_i \rangle$ by the onsite densities n_i in Eq. (2). The solution of Eqs. (3) leads to the following spectrum:

$$E + \mu = Vnz \pm \sqrt{(Vn\tau z)^2 + t_k^2} = Vnz \pm \omega_k. \tag{4}$$

The spectrum defined by (4) resembles the superconductor spectrum, and hence, the first term under the square root is analogous to the superconducting gap squared. In other words, we can introduce the charge-ordering gap by the formula

$$\Delta = Vn\tau z.$$

It depends on the density not only explicitly, but also via the density dependence of τ.

We thus obtain

$$\omega_k = \sqrt{\Delta^2 + t_k^2}. \tag{5}$$

We note a substantial difference between the spectrum of charge-ordered state (5) and the superconducting state: here, the chemical potential does not enter under the square root in (5) for $n \neq 1/2$, which is in contrast to the superconductor spectrum, where

$$\omega_k = \sqrt{(t_k - \mu)^2 + \Delta^2}.$$

We can then find the Green's functions

$$\begin{cases} G_1 = \dfrac{A_k}{E + \mu - Vnz - \omega_k + i0} + \\ \\ \quad + \dfrac{B_k}{E + \mu - Vnz + \omega_k + i0}, \\ \\ G_2 = \dfrac{t_k}{2\omega_k} \dfrac{1}{2\pi} \left[\dfrac{1}{E + \mu - Vnz - \omega_k + i0} - \right. \\ \\ \quad \left. - \dfrac{1}{E + \mu - Vnz + \omega_k + i0} \right], \end{cases} \tag{6}$$

where

$$A_k = \frac{1}{4\pi}\left(1 - \frac{\Delta}{\omega_k}\right), \quad B_k = \frac{1}{4\pi}\left(1 + \frac{\Delta}{\omega_k}\right). \tag{7}$$

After the standard Wick transformation

$$E + i0 \to iE$$

in the expression for G_1, we find the densities

$$\begin{aligned} n_1 &= n(1+\tau) = \\ &= \int \left[\left(1 - \frac{\Delta}{\omega_k}\right) f_F(\omega_k - \mu + Vnz) + \right. \\ &\left. + \left(1 + \frac{\Delta}{\omega_k}\right) f_F(-\omega_k - \mu + Vnz) \right] \frac{d\mathbf{k}}{2\Omega_{BZ}}, \\ n_2 &= n(1-\tau) = \\ &= \int \left[\left(1 + \frac{\Delta}{\omega_k}\right) f_F(\omega_k - \mu + Vnz) + \right. \\ &\left. + \left(1 - \frac{\Delta}{\omega_k}\right) f_F(-\omega_k - \mu + Vnz) \right] \frac{d\mathbf{k}}{2\Omega_{BZ}}, \end{aligned} \tag{8}$$

where

$$f_F(y) = \frac{1}{e^{y/T}+1}$$

is the Fermi distribution function and Ω_{BZ} is the volume of the first Brillouin zone.

Adding and subtracting the two equations for n_1 and n_2, we obtain the resulting system of equations for n and μ:

$$\begin{aligned} 1 &= Vz\int \frac{1}{\omega_k}\left[f_F(-\omega_k-\mu+Vnz) - \right. \\ &\left. - f_F(\omega_k-\mu+Vnz)\right]\frac{d\mathbf{k}}{2\Omega_{BZ}}, \\ n &= \int \left[f_F(-\omega_k-\mu+Vnz)+\right. \\ &\left. + f_F(\omega_k-\mu+Vnz)\right]\frac{d\mathbf{k}}{2\Omega_{BZ}}. \end{aligned} \tag{9}$$

For low temperatures ($T \to 0$) and $n \le 1/2$, it is reasonable to assume that $\mu - Vnz$ is negative. Therefore,

$$f_F(\omega_k-\mu+Vnz) = 0,$$

$$f_F(-\omega_k-\mu+Vnz) = \theta(-\omega_k-\mu+Vnz)$$

is the step function.

It is easy to see that for $n = 1/2$, the system of equations (9) yields identical results for all

$$-\Delta \le \mu - Vnz \le \Delta.$$

From this standpoint, $n = 1/2$ is the indifferent equilibrium point. For infinitely small deviations from $n = 1/2$, that is, for densities $n = 1/2 - 0$, the chemical potential must be defined as

$$\mu = -\Delta + \frac{Vz}{2} = \frac{Vz}{2}(1-\tau).$$

If we consider the strong coupling case $V \gg 2t$ and assume a constant density of states inside the band, we have

$$\tau = 1 - \frac{2W^2}{3V^2z^2},$$

for a simple cubic lattice and therefore,

$$\mu = \frac{W^2}{3Vz}, \tag{10}$$

where $W = 2zt$ is the bandwidth. We note that for the density $n = 1/2$, the charge-ordering gap Δ appears for an arbitrary interaction strength V. This is due to the existence of nesting in our simple model. In the weak coupling case $V \ll 2t$ and with the perfect nesting, we have

$$\Delta \propto W \exp\left\{-\frac{W}{Vz}\right\}$$

and τ is exponentially small. For $Vz \gg W$ or, accordingly, for $V \gg 2t$, it follows that $\Delta \approx Vz/2$ and $\tau \to 1$. As mentioned above, for a general form of the electron dispersion without nesting, the charge ordering exists only if the interaction strength V exceeds a certain critical value of the order of the bandwidth W [2]. In what follows, we restrict ourselves to the physically more instructive strong-coupling case $V \gg 2t$.

For the constant density of states (flat band), the integrals in (9) can be taken explicitly and the system of equations (9) can be easily solved for arbitrary n. We note, however, that in the strong-coupling case $V \gg 2t$ and for small density deviations from $1/2$ ($\delta \ll 1$), the results are not very sensitive to the form of the electron dispersion. That is why we do not need to solve the system of equations (9) exactly.

We now consider the case where $n = 1/2 - \delta$, with $\delta \ll 1$ being the density deviation from $1/2$. In this case, $\mu = \mu(\delta, \tau)$ and we have two coupled equations for μ and τ. As a result,

$$\begin{aligned} \mu(\delta) &\approx Vnz(1-\tau) - \frac{4W^2}{Vz}\delta^2 \approx \\ &\approx \frac{W^2}{3Vz} + \frac{4W^2}{3Vz}\delta + O(\delta^2). \end{aligned} \tag{11}$$

The energy of the charge-ordered state is therefore given by

$$E_{CO}(\delta) = E_{CO}(0) - \frac{W^2}{3Vz}\delta - \frac{2W^2}{3Vz}\delta^2 + O(\delta^3), \tag{12}$$

where

$$E_{CO}(0) = -\frac{W^2}{6Vz}$$

is the energy precisely corresponding to the density $n = 1/2$ and $|E_{CO}(0)| \ll W$. At the same time, the charge-ordering gap Δ is given by

$$\Delta \approx \frac{Vz}{2}\left[1 - 2\delta - \frac{2W^2}{3V^2z^2}(1+4\delta)\right]. \tag{13}$$

The dependence of the chemical potential μ and the total energy E on δ in Eqs. (11) and (12) actually stems from this linear decrease of the energy gap Δ with the deviation from half-filling.

For $n > 1/2$, the energy of the charge-ordered state starts to increase rapidly due to a large contribution of the Coulomb repulsion (the upper Verwey band is partially filled for $n > 1/2$). For $n > 1/2$, contrary to the case where $n < 1/2$, each extra electron put into the checkerboard charge-ordered state necessarily has occupied nearest-neighbor sites, increasing the to-

tal energy by $Vz|\delta|$. For $|\delta| = n - 1/2 > 0$, we then have

$$E_{CO}(\delta) = E_{CO}(0) + \\ + \left(Vz - \frac{W^2}{3Vz}\right)|\delta| - \frac{2W^2}{3Vz}\delta^2 + O(\delta^3). \quad (14)$$

Accordingly, the chemical potential is given by

$$\mu(\delta) = Vz - \frac{W^2}{3Vz} - \frac{4W^2}{3Vz}|\delta| + O(\delta^2). \quad (15)$$

It undergoes a jump equal to Vz as $\tau \to 1$. We note that the gap Δ is symmetric for $n > 1/2$ and is given by

$$\Delta \approx \frac{Vz}{2}\left[1 - 2|\delta| - \frac{2W^2}{3V^2z^2}(1 + 4|\delta|)\right].$$

We could make the entire picture symmetric with respect to $n = 1/2$ by shifting all the one-electron energy levels and the chemical potential by $Vz/2$, i.e., defining

$$\mu' = \mu - Vz/2.$$

In terms of μ', Eqs. (11) and (15) can be written as

$$\mu' = -\frac{Vz}{2} + \frac{W^2}{3Vz} + \frac{4W^2}{3Vz}\delta, \quad n < \frac{1}{2},$$

$$\mu' = \frac{Vz}{2} - \frac{W^2}{3Vz} - \frac{4W^2}{3Vz}|\delta|, \quad n > \frac{1}{2}.$$

Similarly to the situation in semiconductors, we have $\mu' = 0$ precisely at the point $n = 1/2$, which means that the chemical potential lies in the middle of the band gap (see Fig. 1). At densities $n = 1/2 - 0$, the chemical potential $\mu' = -Vz/2$ coincides with the upper edge of the filled Verwey band.

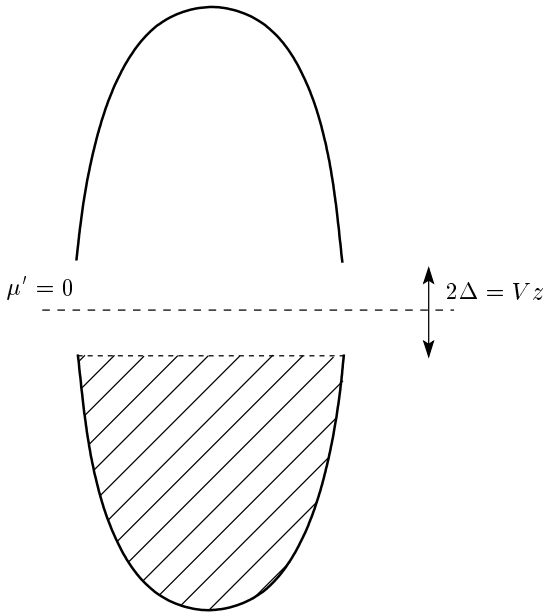

Fig. 1. Band structure of model (1) at $n = 1/2$. The lower Verwey band is completely filled. The upper Verwey band is empty. Chemical potential $\mu' = 0$ lies in the middle of the band gap with the width 2Δ

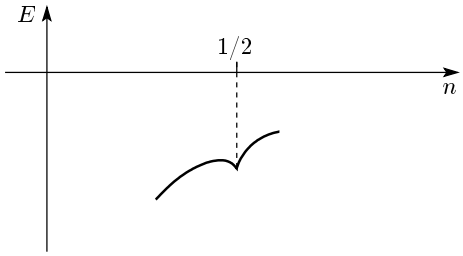

Fig. 2. Energy of the charge-ordered state versus charge density as $n \to 1/2$

3. PHASE SEPARATION

We now check the stability of the charge-ordered state. At the densities close to $n = 1/2$, the dependence of energy on the charge density has the form illustrated in Fig. 2. This figure clearly indicates a possible instability of the charge-ordered state. Indeed, the most remarkable implication of Eqs. (11)–(15) is that the compressibility κ of the homogeneous charge-ordered system is negative for the densities different from 1/2,

$$\frac{1}{\kappa} \propto \frac{d\mu}{dn} = -\frac{d\mu}{d\delta} = \frac{d^2E}{d\delta^2} = -\frac{4W^2}{3Vz} < 0, \quad (16)$$

where $\delta = 1/2 - n$. This is a manifestation of the tendency toward the phase separation characteristic of the charge-ordered system with $\delta \neq 0$. The presence of a kink in $E_{CO}(\delta)$ (cf. Eqs. (12) and (14)) implies that one of the states into which the system might separate would correspond to the checkerboard charge-ordered state with $n = 1/2$, whereas the other would have a certain density n' smaller or larger than 1/2. This conclusion resembles that in [4] (see also [10, 14]), although the detailed physical mechanism is different. The possibility of a phase separation in model (1) away from half-filling was also reported earlier in [12] for the infinite-dimensional case. In what follows, we focus our attention on the situation with $n < 1/2$ (underdoped manganites); the case where $n > 1/2$ apparently has certain special properties — the existence of stripe phases etc. [13], the detailed origin of which is not yet clear.

It is easy to understand the physics of the phase separation in our case. As follows from (13), the charge-ordered gap decreases linearly with the deviation from the half-filling. Correspondingly, the energy of the homogeneous charge-ordered state rapidly increases, and it is more favorable to «extract» extra holes from the charge-ordered state, putting them into one part of the sample, while creating the «pure» checkerboard charge ordering state in the other part. The energy loss due to this redistribution of holes is overcompensated by the gain provided by a better charge ordering.

However, the hole-rich regions would not be completely «empty», similarly to pores (clusters of vacancies) in crystals: we can gain an extra energy by «dissolving» a certain amount of electrons there. In doing this, we decrease the band energy of the electrons due to their delocalization. Thus, this second phase would be a metallic one. The simplest state of this kind is a homogeneous metal with the electron concentration n_m. This concentration, as well as the relative volume of the metallic and charge-ordered phases, can be easily calculated by minimizing the total energy of the system. The energy of the metallic part of the sample E_m is given by

$$E_m = -tzn_m + ct(n_m)^{5/3} + V(n_m)^2, \qquad (17)$$

where c is a constant.

Minimizing (17) with respect to n_m, we find the equilibrium electron density in the metallic phase. For the strong coupling case $V > zt$, we obtain (neglecting a relatively small correction provided by the term with $(n_m)^{5/3}$)

$$n_{m0} \approx tz/2V. \qquad (18)$$

In accordance with this simple treatment, the system with $n_{m0} < n < 1/2$ would therefore undergo the phase separation into the charge-ordered phase with $n = 1/2$ and the metallic phase with $n = n_{m0}$. For arbitrary n, the relative volumes v_m and v_{CO} of these phases can be found from the Maxwell construction,

$$\frac{v_m}{v_{CO}} = \frac{1/2 - n}{n - n_{m0}}, \qquad (19)$$

which implies that the metallic phase occupies the part v_m of the total volume v given by

$$\frac{v_m}{v} = \frac{1/2 - n}{1/2 - n_{m0}}. \qquad (20)$$

The metallic phase occupies the entire sample when the total electron density n is less than n_{m0}.

4. AN EXAMPLE: THE PHASE SEPARATED STATE WITH METALLIC DROPLETS

As argued above, the system with a short-range repulsion described by Eq. (1) is unstable with respect to the phase separation for n close to but different from $1/2$. The long-range Coulomb forces, however, prevent the full phase separation into large regions containing all extra holes and the pure $n = 1/2$ charge-ordered region. We can avoid this energy loss by forming, instead of one big metallic phase with many electrons, finite metallic clusters with fewer electrons. The limiting case would be a set of spherical droplets, each containing one electron. This state is similar to magnetic polarons («ferrons») considered in the phase separation problem for doped magnetic insulators [8, 14, 11].

We now estimate the characteristic parameters of these droplets. The main purpose of this treatment is to demonstrate that the energy of the state constructed in this way is lower than the energy of the homogeneous state, even if we treat these droplets rather crudely and do not optimize all their properties. In particular, we make the simplest assumption that the droplets have sharp boundaries and that the charge-ordered state existing outside these droplets is not modified in their vicinity. This state can be treated as a variational one: optimizing the structure of the droplet boundary can only decrease its energy.

The energy (per unit volume) of the droplet state with the concentration of droplets n_d can be written in total analogy with the ferron energy in the double-exchange model (see [14, 11]). This yields

$$E_{droplet} = -tn_d\left(z - \frac{\pi^2 a^2}{R^2}\right) - \\ - \frac{W^2}{6Vz}\left[1 - n_d\frac{4}{3}\pi\left(\frac{R}{a}\right)^3\right], \qquad (21)$$

where a is the lattice constant and R is the droplet radius. The first term in (21) corresponds to the kinetic energy gain of the electron delocalization inside the metallic droplets and the second term describes the charge ordering energy in the remaining insulating part of the sample.

Minimization of the energy in (21) with respect to R gives

$$\frac{R}{a} \approx \left(\frac{2V}{t}\right)^{1/5}. \qquad (22)$$

The critical concentration n_{dc} corresponds to the configuration where metallic droplets start to overlap,

i.e., where the volume of the charge-ordered phase (the second term in (21)) tends to zero. Hence,

$$n_{dc} = \frac{3}{4\pi}\left(\frac{a}{R}\right)^3 \propto \left(\frac{t}{V}\right)^{3/5}. \qquad (23)$$

Actually, one should include the surface energy contribution to the total energy of the droplet. The surface energy must be of the order W^2R^2/V. For large droplets, this contribution is small compared to the term $\propto R^3$ in (21); it would also be reduced for a «soft» droplet boundary. It is easy to show that even in the worst case of a small droplet (of the order of several lattice constants) with a sharp boundary, R/a acquires the factor $1 - 0.2(t/2V)^{1/5}$ related to the surface contribution. Thus, the corrections related to the surface would not exceed about 20% of the bulk value. That is why we ignore this term below.

Comparing (12) with (21) and (22), we see that for the deviations from half-filling such that

$$0 < \delta \le \delta_c = 1/2 - n_{dc},$$

the energy of the phase-separated state is always lower than the energy of the homogeneous charge-ordered state. The energy of the droplet state (21) with the radius given by (22) is also lower than the energy of the fully phase-separated state obtained by the Maxwell construction from homogeneous metallic state (17). Correspondingly, the critical concentration n_{dc} in Eq. (23) is larger than n_{m0} in Eq. (18). There is no contradiction here: in the droplet state that we constructed, the electrons are confined to spheres of the radius R, and even when these droplets start to overlap at $n = n_{dc}$, occupying the entire sample, the electrons, by construction, are still confined within their own spheres and avoid each other. In other words, a certain degree of charge-ordering correlations is still present in our droplet state, decreasing the repulsion and hence the total energy.

Thus, the energy of the phase-separated state with the droplets corresponds to the global minima of the energy for all $0 < \delta \le \delta_c$. This justifies our conclusion about the phase separation into the charge-ordered state with $n = 1/2$ and a metallic state with small spherical droplets.

The situation encountered here resembles that of a partially filled strongly interacting Hubbard model, with the charge-ordered state corresponding to the antiferromagnetic state of the latter and with the nearest-neighbor interaction V playing the role of Hubbard's U. In both cases, the kinetic energy of doped carriers tends to destroy this «antiferro» or charge ordering, by first «spoiling» it in their vicinity and eventually leading to the formation of the metallic state (Nagaoka ferromagnetism). In the Hubbard model, we also face the situation with the phase separation at a sufficiently small doping [21].

We also note that for $n > 1/2$, the compressibility of the charge-ordered state is again negative,

$$\frac{1}{\kappa} = \frac{d^2E}{d\delta^2} = -\frac{4W^2}{3Vz} < 0,$$

and has the same value as for $n < 1/2$. As a result, it is again more favorable to create a phase-separated state for these densities. However, as already mentioned, the nature of the second phase with $n > 1/2$ is not quite clear at present, and therefore, we do not consider this case here.

5. AN EXTENDED MODEL

We can now extend the model discussed in the previous sections by taking the essential magnetic interactions into account. In manganites, in addition to the conduction electrons in the e_g bands, there also exist practically localized t_{2g} electrons, which we now include in our consideration. The corresponding Hamiltonian is given by

$$\hat{H} = -t\sum_{\langle i,j\rangle,\sigma} c^+_{i\sigma}c_{j\sigma} + V\sum_{\langle i,j\rangle} n_i n_j - J_H\sum_i \mathbf{S}_i\sigma_i + J\sum_{\langle i,j\rangle}\mathbf{S}_i\mathbf{S}_j - \mu\sum_i n_i. \qquad (24)$$

In comparison to (1), the additional terms here correspond to the strong Hund-rule onsite coupling J_H between the localized spins $\mathbf{S}$ and the spins of conduction electrons σ, and a relatively weak Heisenberg antiferromagnetic (AFM) exchange J between neighboring local spins. In real manganites, the AFM ordering of the zigzag (CE) type in the charge-ordered phase is determined not only by the exchange of the localized t_{2g} electrons but to a large extent, by the charge- and orbitally-ordered e_g electrons themselves. For simplicity, we ignore this factor and assume the superexchange interaction to be the same in the charge-ordered and in the metallic phases.

It is physically reasonable to consider this model in the limit

$$J_H S > V > W > JS^2.$$

In the absence of the Coulomb term, this is exactly the conventional double-exchange model (see, e.g., [8, 14]).

As it is usually assumed in the theory of the double exchange (that is, in the theory where $J_H \gg W$), the main role of the itinerant electrons is to form a parallel arrangement of local spins. The exchange-correlation effects of the itinerant electrons themselves are not very important here and can be included in the renormalization of the effective bandwidth.

We note that the absence of doubly occupied sites in (24) is guaranteed by the large Hund's term. It also favors the metallicity in the system, because the effective bandwidth depends on the magnetic order in our problem. The estimate for the critical concentration is therefore different from the one in (23). Similarly to [14], the metallic droplets are ferromagnetic (FM) because of the double exchange. The energy of one such droplet is given by

$$E = -t\left(z - \frac{\pi^2 a^2}{R^2}\right) - \frac{W^2}{6Vz}\left[1 - \frac{4}{3}\pi\left(\frac{R}{a}\right)^3\right] + \\ + zJS^2\frac{4}{3}\pi\left(\frac{R}{a}\right)^3 - zJS^2\left[1 - \frac{4}{3}\pi\left(\frac{R}{a}\right)^3\right]. \quad (25)$$

The last two terms in (25) describe the loss of the Heisenberg AFM exchange energy inside the FM metallic droplets and the gain of this energy in the AFM insulating part of the sample, respectively. The minimization with respect to the droplet radius (as in (21)) yields

$$\frac{R}{a} \propto \left(\frac{t}{V} + \frac{JS^2}{t}\right)^{-1/5}. \quad (26)$$

We note that at $t/V \ll JS^2/t$, Eq. (26) gives the same estimate for the radius of a FM metallic droplet

$$\frac{R}{a} \sim \left(\frac{t}{JS^2}\right)^{1/5}$$

as in [8, 14].

In the opposite limit where $t/V \gg JS^2/t$, we reproduce the same result

$$\frac{R}{a} \sim \left(\frac{V}{t}\right)^{1/5}$$

as in (22). Finally, the critical concentration n_c is estimated as

$$n_c \propto \left(\frac{t}{V} + \frac{JS^2}{t}\right)^{3/5}. \quad (27)$$

As a result, also taking the tendency to the phase separation at very small values of n into account [8–11, 14], we arrive at the following phase diagram for the extended model (cf. [11]):

1. At $0 < n < \left(JS^2/t\right)^{3/5}$, it corresponds to the phase separation into a FM metal with $n = n' > 0$ embedded into the AFM insulating matrix ($n = 0$). To minimize the Coulomb energy, it may again be favorable to split this metallic region into droplets with the concentration n' and the average radius given by Eq. (26) with $t/V = 0$, each containing one electron and kept apart from one another.

2. At $\left(JS^2/t\right)^{3/5} < n < \left(t/V + JS^2/t\right)^{3/5} < 1/2$, the system is a FM metal. Of course, we need a window of parameters to satisfy the inequality in the right-hand side. In actual manganites, where $t/V \sim 1/2$–$1/3$ and $JS^2/t \sim 0.1$, these conditions imposed on n are not necessarily satisfied. Experiments suggest that this window is present for $La_{1-x}Ca_xMnO_3$, but it is definitely absent for $Pr_{1-x}Ca_xMnO_3$ [11].

3. Finally, at $\left(t/V + JS^2/t\right)^{3/5} < n < 1/2$, we have the phase separation in the form of FM metallic droplets inside the AFM charge-ordered matrix.

This phase diagram is in a good qualitative agreement with many available experimental results for real manganites [22–25], in particular with the observation of the small-scale phase separation close to the doping 0.5 [26]. We also note that our phase diagram has certain similarities with the phase diagram obtained in [27, 28] for the problem of spontaneous ferromagnetism in doped excitonic insulators.

6. CONCLUSIONS

Summarizing, we have shown that the narrow-band system that has the checkerboard charge ordering at $n = 1/2$ (corresponding to the doping $x = 0.5$) is unstable toward phase separation away from half-filling ($n \neq 1/2$). The system separates into regions with the ideal charge ordering ($n = 1/2$) and other regions where extra electrons or holes are trapped. The simplest form of these metallic regions could be spherical metallic droplets embedded into the charge-ordered insulating matrix. Simple considerations allow estimating the size of these droplets and the critical concentration, or doping $x_c = 1/2 - \delta_c$, at which the metallic phase occupies the entire sample and the charge-ordered phase disappears. The account of the magnetic interactions does not change these conclusions but somewhat modifies the characteristic parameters of the metallic droplets.

The long-range Coulomb interaction may also modify the results, but we do not expect any qualitative changes. For realistic values of the parameters, the size

of metallic droplets is still microscopic (about 10 Å) and the excess charge contained in them is rather small.

The obtained picture corresponds rather well to the known properties of $3D$ and layered manganites close to (less than) half doping, $x \leq 1/2$. The percolation picture of transport properties emerging from this treatment is confirmed by the results reported in [7, 15, 22, 24–26]; moreover, the coexistence of ferromagnetic reflections and those of the CE type magnetic structure typical of the charge-ordered state at $x = 0.5$ were observed by the neutron scattering [29]. Thus, the general behavior of the underdoped manganites ($x \leq 0.5$) is in a good qualitative agreement with our results.

Our treatment also leads to the same tendency to the phase separation (instability of the homogeneous charge-ordered phase) for the overdoped regime $x > 0.5$. It is still not clear what would be the second phase in this case. Therefore, we did not concentrate our attention on this case.

Our treatment is also applicable to other systems with the charge ordering, such as cobaltites [18] and nickelates [19]. It would be interesting to study them for charge carrier concentrations different from the commensurate «checkerboard» one.

A number of important problems still remain unresolved (the origin of the «in-phase» ordering along the c-direction in perovskite manganites, the detailed description of inhomogeneous states in the overdoped regime $x > 1/2$, and the behavior at finite temperatures). Nevertheless, in spite of the introduced simplifications, our model seems to capture the essential physics underlying the interplay between phase separation and charge ordering in transition metal oxides.

We are grateful to N. M. Plakida and M. S. Mar'enko for stimulating discussions. D. Kh. expresses gratitude to S.-W. Cheong and Y. Moritomo for discussions of the experimental aspects of the problem. The work was supported by INTAS (grants № 97-0963 and 97-11954), the Russian Foundation for Basic Research (projects № 00-02-16255 and 00-15-96570), and by the Russian–Dutch Program for Scientific Cooperation funded by the Netherlands Organization for Scientific Research (NWO). M. Yu. K. acknowledges the support of the Russian President Program (grant № 96-15-9694). The work of D. Kh. was also supported by the Netherlands Foundation for the Fundamental Research of Matter (FOM) and by the European network OXSEN.

REFERENCES

1. E. Verwey, Nature (London) **144**, 327 (1939); E. Verwey and P. W. Haayman, Physica **8**, 979 (1941).
2. D. I. Khomskii, Preprint of the P. N. Lebedev Physics Institute № 105 (1969).
3. T. Mutou and H. Kontani, Phys. Rev. Lett. **83**, 3685 (1999).
4. J. van den Brink, G. Khaliullin, and D. Khomskii, Phys. Rev. Lett. **83**, 5118 (1999).
5. G. Jackeli, N. B. Perkins, and N. M. Plakida, Phys. Rev. B **62**, 372 (2000).
6. Z. Jirák, S. Krupička, Z. Šimša et al., J. Magn. Magn. Mater. **53**, 153 (1985).
7. A. Arulraj, A. Biswas, A. K. Raychaudhuri, et al., Phys. Rev. B **56**, R8115 (1998); M. Uehara, S. Mori, C. H. Chen, and S.-W. Cheong, Nature **399**, 560 (1999).
8. E. L. Nagaev, Usp. Fiz. Nauk **166**, 833 (1996).
9. A. Moreo, S. Yunoki, and E. Dagotto, Science **283**, 2034 (1999).
10. D. Arovas and F. Guinea, Phys. Rev. B **58**, 9150 (1998).
11. D. I. Khomskii, Physica B **280**, 325 (2000).
12. G. S. Uhrig and R. Vlamink, Phys. Rev. Lett. **71**, 271 (1993).
13. S. Mori, C. H. Chen, and S.-W. Cheong, Nature (London) **392**, 473 (1998).
14. M. Yu. Kagan, D. I. Khomskii, and M. V. Mostovoy, Eur. Phys. J. B **12**, 217 (1999).
15. L. P. Gor'kov and V. Z. Kresin, Pis'ma v ZhETF **67**, 985 (1998).
16. S. Yunoki, T. Hotta, and E. Dagotto, Phys. Rev. Lett. **84**, 3714 (2000).
17. I. V. Solov'ev and K. Terakura, Phys. Rev. Lett. **83**, 2825 (1999).
18. Y. Moritomo, M. Takeo, X. J. Liu et al., Phys. Rev. B **58**, R13334 (1998).
19. J. A. Alonso, J. L. García-Muñoz, M. T. Fernández-Díaz et al., Phys. Rev. Lett. **82**, 3871 (1999).
20. P. Pietig, R. Bulla, and S. Blawid, Phys. Rev. Lett. **82**, 4046 (1999).
21. P. B. Visscher, Phys. Rev. B **10**, 943 (1974).

22. N. A. Babushkina, L. M. Belova, A. N. Taldenkov et al., J. Phys.: Condens. Matter **11**, 5865 (1999).

23. M. Hennion, F. Moussa, G. Biotteau et al., Phys. Rev. Lett. **81**, 1957 (1998).

24. G. Allodi, R. De Renzi, G. Guidi et al., Phys. Rev. B **56**, 6036 (1997).

25. I. F. Voloshin, A. V. Kalinov, S. E. Savel'ev et al., Pis'ma v ZhETF **71**, 157 (2000).

26. Y. Moritomo, A. Machidas, S. Mori et al., Phys. Rev. B **60**, 9220 (1999).

27. L. Balents and C. M. Varma, Phys. Rev. Lett. **84**, 1264 (2000).

28. V. Barzykin and L. P. Gor'kov, Phys. Rev. Lett. **84** 2207 (2000).

29. R. Kayumoto, H. Yoshizawa, H. Kawano et al., Phys. Rev. B **60**, 9506 (1999).